Received 19 October 2025; Accepted 12 November 2025
https://doi.org/10.48612/letters/2025-4-362-368
https://elibrary.ru/lkezeq

DFT-based parameterization of a non-orthogonal tight-binding model for electronic band structure calculations of carbon and hydrocarbon materials

N. V. Kryakvin[1], V. A. Kurakin[†1], T. N. Kobernik[2], M. M. Maslov[1]

[†]fromkurakin@mail.ru

[1]Laboratory of 2D Nanomaterials in Electronics, Photonics and Spintronics, National Research Nuclear University "MEPhI", Moscow 115409, Russia
[2]Energy Technology Center, Skolkovo Institute of Science and Technology, Moscow 121205, Russia

Abstract: The tight-binding model provides a useful alternative to first-principles methods for quantum mechanical modeling of atomic structures and the physicochemical properties of materials. It is well-suited for investigating topologically complex systems with large numbers of atoms, since it substantially reduces the computational cost. However, the accuracy of the tight-binding model critically depends on the choice of parameters. In this work, we introduce a parameterized, non-orthogonal tight-binding model to calculate the electronic properties of carbon and hydrocarbon materials. We performed the parameterization using initial DFT calculations of the electronic band structures of seven carbon and hydrocarbon materials with different dimensionalities and atomic hybridizations. The calculated electronic band structures show reasonable agreement with DFT results. The proposed parameter set is transforable and suitable for different hydrocarbon crystals. As a result, the represented approach can support extensive searches for new materials of this type, as well as more efficient and accurate studies of the electronic band structures of their synthesized counterparts. Furthermore, such synthesis of methods allows the analytical advantages of tight-binding method to be retained while complementing them with the accuracy of *ab initio* calculations. Thus, this work should contribute to significant improvements in the key performance characteristics of computational materials science methodologies and algorithms.

Keywords: non-orthogonal tight-binding model, DFT-based parameterization, electronic band structure, carbon nanomaterials, graphene

Acknowledgements: *The work was supported by the Ministry of Science and Higher Education of the Russian Federation, project FSWU-2024-0014.*

1. Introduction

Carbon is one of the most essential elements in nature, playing a leading role in modern science, engineering, medicine, industry, and agriculture [1]. The peculiarity of its structure allows carbon to form crystal structures, existing in states with different types of hybridization (sp, sp^2, sp^3), which is confirmed by the existence of zero-dimensional (0D) carbon fullerenes [2] and quantum dots [3], one-dimensional (1D) carbon nanotubes [4], chains [5] and polyprismanes [6], two-dimensional (2D) graphene [7] and penta-graphene [8], three-dimensional (3D) metallic [9] and superhard [10] carbons. In addition, there are purely carbon-based atomic structures encompassing nanosystems of various dimensionalities. A striking example of such structures is the carbon "peapods" [11], composed of 0D and 1D nanostructures.

Many of the materials mentioned above exhibit an exceptionally wide spectrum of electromagnetic properties, — ranging from insulating and semiconducting to metallic and even superconducting. Metallic carbon, in particular, has been shown to demonstrate phonon-plasmon coupling [12], negative differential resistance [13], superconductivity [14, 15], and excellent performance as an anode material for lithium-ion batteries [16]. Moreover, this form of carbon may exhibit magnetic behavior when the Stoner criterion is fulfilled [17], and, owing to its high density of states (DOS) at the Fermi level, it can function as an efficient catalyst [18].

Unlike conventional semiconductors such as silicon, carbon-based materials provide a unique degree of flexibility in tailoring their electronic properties through changes in atomic hybridization within compounds. Hydrocarbon (H–C) derivatives are particular interest, as the incorporation of hydrogen into carbon systems alters atomic hybridization, thereby affecting their electromagnetic properties. For instance, the hydrogenation-induced transition from sp^2 to sp^3 hybridization in graphene drastically modifies its electron transport behavior, transforming it from a semimetal into a semiconductor [19] or even into a dielectric (when fully covered with hydrogen, turning graphene into graphane [20]). This characteristic clearly differentiates carbon materials from those based on other chemical elements, where comparable modifications typically require complex doping procedures and additional external interventions.

A wide range of physicochemical properties of carbon-based materials has allowed them to successfully establish a strong presence in various next-generation high-tech applications. Carbon nanostructures such as graphene, graphane, graphyne, and carbon nanotubes are already being extensively employed in fields including nanoelectronics [21,22], spintronics [23,24], and flexible electronics [25,26]. These examples highlight the importance of developing diverse carbon systems with tunable electronic properties. At the same time, advancing efficient and accurate methods for calculating these properties remains a critically important task.

The extraordinary electromagnetic properties of carbon systems are governed by their electronic structures, which can be reliably computed using density functional theory (DFT) [27] with appropriate corrections such as LDA+U [28] or various hybrid functionals [29,30]. Nevertheless, accurate determination of electronic structures with DFT software packages typically demands substantial computational resources in terms of both time and memory. This is particularly challenging for complex crystalline architectures, as well as for non-crystalline or quasicrystalline systems. For these reasons, among the vast number of diverse allotropic forms of carbon, electronic structures have so far been calculated for only a limited subset. For instance, in the SACADA database [31], out of 5223D carbon allotropes, only 207 structures have reported band gap values. In reality, far more diverse allotropic modifications of carbon exist, which can be formed by different combinations of *sp*, sp^2, sp^3 hybridizations of atoms within them with greater topological complexity, which poses significant obstacles for calculating electronic structures of such systems [32].

The tight-binding method (TBM) requires substantially less computational power for evaluating the electron transport properties of materials, while still providing an efficient framework for modeling the electronic behavior of various atomic structures [33,34]. This approach is particularly valuable for analyzing π-electron systems such as graphene, where the electronic band structure (EBS) near the Dirac point can be accurately captured using simple tight-binding (TB) Hamiltonians [35,36]. For hydrogenated derivatives of graphene, TBM can be modified to account for changes in atomic hybridization of such materials and the effects of hydrogen on their electronic behavior. Nevertheless, TBM has its limitations, the most significant being that TB Hamiltonians are typically constructed on the basis of empirically fitted parameter values [37,38].

In recent years, machine learning (ML) techniques have been increasingly employed in computational materials science as a means of striking a balance between accuracy and computational efficiency [39–45]. Nevertheless, applying such approaches to quantum-mechanical modeling of electronic properties requires large training datasets [46], and consequently their reliability may be reduced for more exotic structures. Moreover, although ML has been actively and successfully utilized for predicting and classifying crystal structures [39,41], its accuracy in estimating material band gap values can be limited [40]. Therefore, the pursuit of a compromise between accuracy and efficiency in calculating the electron transport properties of various systems remains relevant.

In this work, we report calculations of the EBSs of carbon and H–C materials with different dimensionalities and atomic hybridizations, including graphene, graphane, γ1-graphyne-1, (5,0) and (5,5) single-walled carbon nanotubes (SWCNTs), and diamane with AA- and AB-type atomic stacking. The calculations are carried out using a parameterized non-orthogonal tight-binding model (NTBM), and the accuracy of this approach is assessed by comparison with corresponding DFT results.

2. Materials and methods

The non-orthogonal tight-binding model (NTBM) employed in this study has been previously applied on numerous occasions to investigate the electronic, energetic, optical, and other properties of various carbon and H–C materials, such as graphane nanoribbons [47], carbon peapods [48], and SWCNTs [49]. The methodology for performing calculations with this model is described in detail in [50,51], where the NTBM parameters were fitted to reproduce the bond energies and topologies of the simulated systems. In the present work, we restrict ourselves to outlining only the key principles and formulas of this methodology as applied to carbon and H–C atomic structures.

For $H_{i\alpha}^{j\beta}$, the following parameterization was employed (a similar parameterization was previously applied in [50,51]):

$$H_{i\alpha}^{j\beta} = \frac{1}{2} K_{ij} S_{i\alpha}^{j\beta} (H_\alpha + H_\beta), \quad (1)$$

where

$$K_{ij} = \begin{cases} 1, i = j \\ K_{ij}^0 e^{-\delta_{ij} R_{ij}}, \ i \neq j \end{cases} \quad (2)$$

(note that $H_{i\alpha}^{j\beta} = H_\alpha$ at $\alpha = \beta$ and $H_{i\alpha}^{j\beta} = 0$ at $\alpha \neq \beta$ since $S_{i\alpha}^{j\beta} = \delta_{\alpha\beta}$). Here, *i* and *j* correspond to atoms, and α and β correspond to orbitals.

As noted in [50], analysis of a hydrocarbon system requires specifying three distinct parameters H_α according to the number of valence atomic orbitals of the chemical elements of such a system (α = 1*s* for hydrogen, α = 2*s* and $2p_x$, $2p_y$, $2p_z$ for carbon), as well as three distinct parameters for each of K_{ij}^0 and δ_{ij} corresponding to the combinations of different atoms in the pairs *ij* (*ij* = HH, CH, CC) within the system. The values of $S_{i\alpha}^{j\beta}$ was evaluated with Roothaan formulas [50,51].

Thus, NTBM combines the relative simplicity of the mathematical framework with the ability to analytically examine the EBSs of materials calculated using this model. Nevertheless, as noted above, the accuracy of TBM calculations is critically dependent on the appropriate choice of parameter values, and the most accurate and reliable approach to determining these values is through parameterization based on *ab initio* calculations (in particular, DFT), which account for electron — electron interactions from first principles, thereby ensuring the physical reliability of the results while retaining the computational efficiency of TBM. In this work, the parameterization procedure was carried out in several stages.

In the first stage, DFT calculations of the EBSs were carried out for the carbon and H–C systems under study, and the corresponding energy levels and electron density

distributions were obtained. All calculations were performed using the Quantum Espresso software package, which is specifically designed for first-principles calculations and employs the Vanderbilt pseudopotential method [52] together with a plane-wave basis set expansion within the local density approximation formalism [53, 54]. For each material studied, particular attention was devoted to the locations of its high-symmetry points in the first Brillouin zone. For 1D and 2D nanosystems, a 2 nm vacuum space was added in the corresponding directions to avoid any interaction of the system with its periodical images.

In the second stage, the values of the above-mentioned parameters H_α, K_{ij}^0, δ_{ij}, ξ_{1s}, ξ_{2s}, ξ_{2p} were optimized. As noted above, the total number of NTBM parameters in this study amounted to 12. These parameters were determined by minimizing the function D, defined as the sum of squared relative deviations between the electronic energies in the valence and conduction bands obtained from NTBM and the corresponding DFT data:

$$D = \sum_{n,k} (U_{n,k}^{\mathrm{DFT}} - U_{n,k}^{\mathrm{NTBM}})^2, \qquad (3)$$

where the summation extends over $n = 2$ bands (valence and conduction bands) and over 121 k-points in the first Brillouin zone. To identify the global minimum of the function D, we employed the gradient descent method. More sophisticated minimization strategies, such as genetic algorithms, can be more effective and accurate in exploring high-dimensional parameter spaces, though they demand significantly larger computational resources [55]. The results of calculations presented in the following section of this work demonstrate that the gradient descent method alone is sufficient for addressing our problem.

Following the parameterization procedure described above, we examined the consistency between the EBSs obtained from the initial DFT calculations and the corresponding NTBM results. Particular attention was devoted to the regions near the Fermi level, as they are crucial for the electron transport properties of materials. In addition, we assessed the accuracy with which NTBM reproduces the global features of each calculated EBS, such as the linear energy spectrum of graphene. All systems were fully relaxed before the EBS-calculations.

3. Results and discussions

This section presents the results of the NTBM parameterization described above for carbon and H–C materials, along with a comparison between the EBSs of seven materials computed using this model and the corresponding data obtained from DFT calculations. In the concluding part of this section, we assess the accuracy of our NTBM calculations in order to identify the optimal conditions for its application.

As mentioned in the previous section of this work, in order to accurately reproduce the EBSs of carbon and H–C systems using the NTBM, we optimized 12 parameters — H_α, K_{ij}^0, δ_{ij}, ξ_{1s}, ξ_{2s}, ξ_{2p} — with the gradient descent method, accounting for interatomic interactions in these systems. Tables 1 and 2 summarize the parameter values obtained from the initial DFT calculations of the EBSs for graphene, graphane, γ1-graphyne-1, (5,0) and (5,5) SWCNTs, and diamane with AA- and AB-type stacking. For each of these materials, the parameter sets listed in the tables provide the closest agreement between the NTBM and DFT EBSs. For ease and clarity of comparison, Tables 1 and 2 also include the corresponding parameter values reported in [51].

When comparing the NTBM parameter values reported in this work with those from [51], it may be noted that some parameters (e.g., H_{ns} values) remain largely unchanged between the two studies, whereas others (e.g., δ values) differ by several orders of magnitude. We suggest that this arises from the essentially empirical, "fitting" nature of these parameters, which causes them to lose their original physical significance.

Figures 1–5 present the calculated EBSs for graphene, graphane, γ1-graphyne-1, (5,0) and (5,5) SWCNTs, and diamane with AA- and AB-type atomic stacking. In these figures, each EBS obtained using the NTBM parameterized as described above is compared with its corresponding DFT counterpart. We believe that such a comparative analysis provides the most straightforward and illustrative way to assess the accuracy of this model.

The EBSs of graphene shown in Fig. 1, obtained using the parameterized NTBM and DFT, exhibit reasonably good agreement near the K point, where graphene is expected to display linear band dispersion and a zero band gap. However, discrepancies arise in other regions of the first Brillouin zone; for instance, between the Γ and M points, as well as between M and K, the NTBM overestimates the valence band energy.

For graphane (Fig. 2), the NTBM described above successfully reproduces the presence of a relatively wide (≈4 eV) band gap, in good agreement with the corresponding DFT calculation. Nevertheless, a minor discrepancy appears near the K point between the considered EBSs, which may be attributed to an incomplete consideration of the influence of

Table 2. Values of parameters describing the interactions between the hydrogen and carbon atoms.

Interaction	K_0		δ (Å^{-1})	
	Present work	Ref. [51]	Present work	Ref. [51]
H–H	1.79	1.85	0.31	0.13
H–C	3.86	1.79	5.15×10^{-5}	1.44×10^{-2}
C–C	3.55	2.67	3.99×10^{-5}	1.62×10^{-1}

Table 1. Values of parameters for the hydrogen and carbon atoms (n is the principal quantum number).

Chemical element	n	ξ_{ns} (Å^{-1})		H_{ns} (eV)		ξ_{ns} (Å^{-1})		H_{np} (eV)	
		Present work	Ref. [51]	Present work	Ref. [51]	Present work	Ref. [51]	Present work	Ref. [51]
H	1	5.33	2.46	−10.45	−10.7	–	–	–	–
C	2	3.92	2.99	−16.14	−16.16	3.15	3.86	−4.15	−10.08

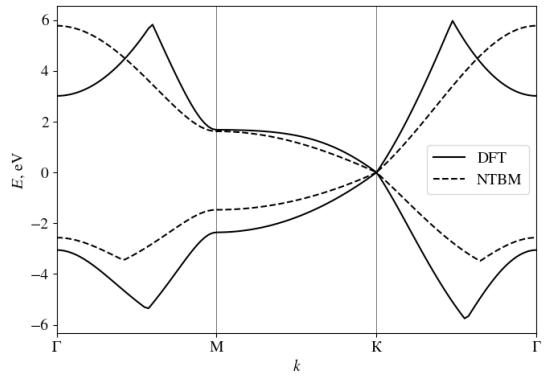

Fig. 1. EBSs of graphene. Solid and dashed lines correspond to DFT and NTBM calculations, respectively.

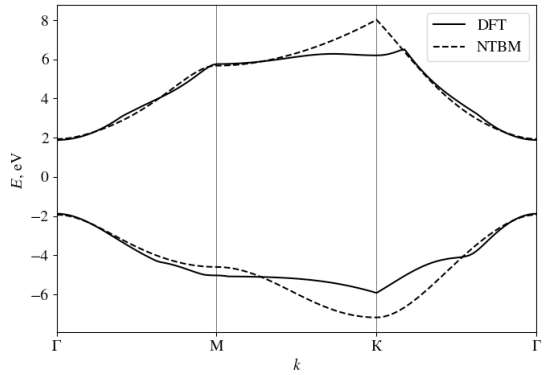

Fig. 2. EBSs of graphane. Solid and dashed lines correspond to DFT and NTBM calculations, respectively.

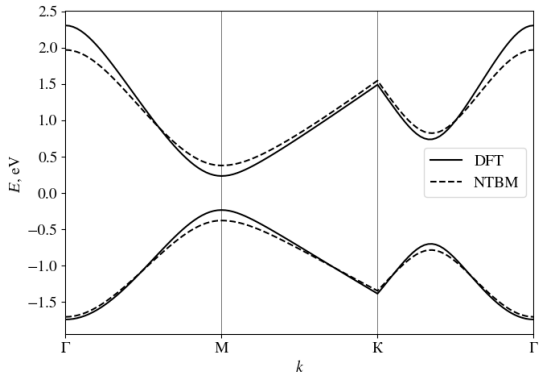

Fig. 3. EBSs of γ1-graphyne-1. Solid and dashed lines correspond to DFT and NTBM calculations, respectively.

hydrogen atoms on the electronic properties of H–C systems modeled with this NTBM.

The EBSs of γ1-graphyne-1 shown in Fig. 3 reveal several key features. Unlike graphene, the DFT calculation of γ1-graphyne-1 exhibits a small (≈0.5 eV) band gap near the M point. Our parameterized NTBM qualitatively reproduces this effect, though it slightly overestimates the gap (to ≈0.8 eV) relative to the DFT result. Furthermore, in the NTBM-based EBS, the valence and conduction bands near the M point display less pronounced curvature compared to their DFT counterparts. At the K point, however, reasonably good agreement is observed between the two approaches to quantum-mechanical modeling of the electron transport properties of this material, supporting the validity of the basic NTBM parameterization. In addition, the band gap of γ1-graphyne-1 is considerably narrower than that of graphane, while its band dispersion retains a partially "graphene-like" character in calculations of the EBS of this system using both of the methods considered in this work. We suggest that the discrepancies near the K point between the results of the NTBM and DFT calculations of the EBSs of γ1-graphyne-1 are less pronounced than in graphane because sp^2 hybridization of carbon atoms dominates in γ1-graphyne-1, as in graphene.

Figure 4 shows the EBSs of diamane with AA- and AB-type atomic stacking, initially obtained from DFT calculations, exhibit relatively wide (≈3 eV) band gaps, which is a common feature of sp^3-hybridized carbon structures. Our parameterized NTBM provides a reasonable description of the overall features of the energy spectra of this material, although certain shifts of the valence and conduction bands appear in the first Brillouin zone compared to the corresponding DFT results. Furthermore, the NTBM underestimates the band gap values of diamane relative to the original DFT calculations, reducing them to ≈2 eV.

Figure 5 clearly shows that the NTBM described above, similar to DFT, accurately predicts the well-known electronic properties of SWCNTs, which depend on their chirality and surface curvature of each of them [56]. Specifically, the zigzag (5,0) SWCNT, although the number 5 is not divisible by 3, turned out to be quasi-metallic rather than semiconducting due to its small diameter, with a band gap of ≈0.1 eV. In contrast, the armchair (5,5) SWCNT exhibited its expected metallic character with a zero band gap. However, near the

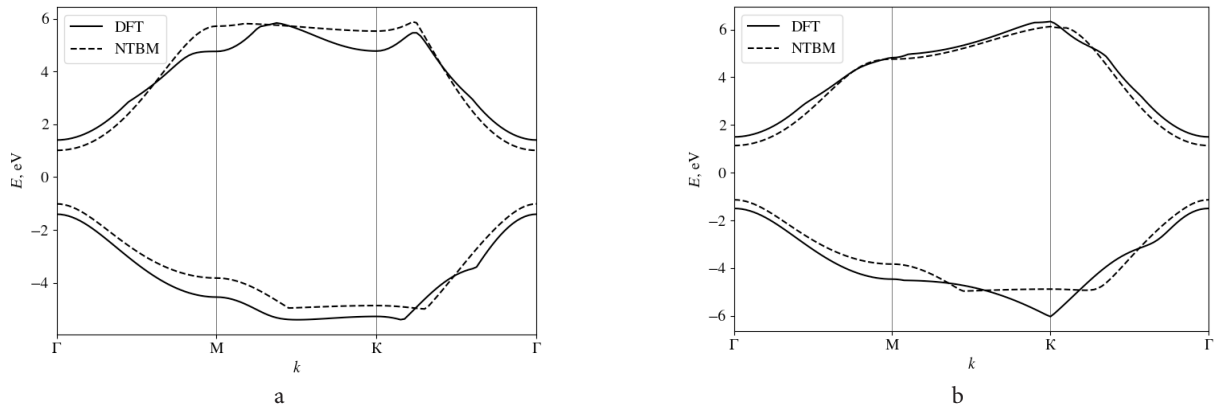

a b

Fig. 4. EBSs of diamane with AA (a) and AB (b) atomic stacking. Solid and dashed lines correspond to DFT and NTBM calculations, respectively.

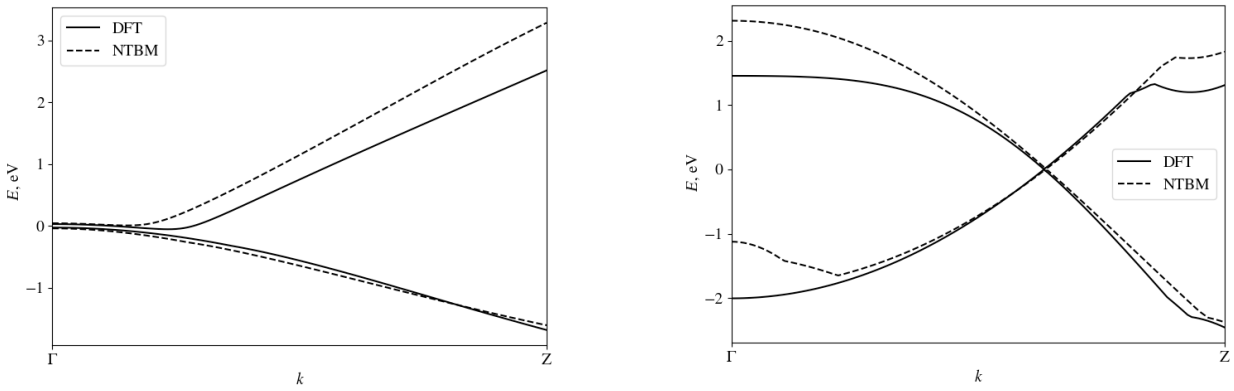

Fig. 5. EBSs of (5,0) (a) and (5,5) (b) SWCNTs. Solid and dashed lines correspond to DFT and NTBM calculations, respectively.

Z point in the (5,0) SWCNT and around the Γ and Z points in the (5,5) SWCNT, we observed discrepancies between the NTBM energy levels and their DFT counterparts. These deviations may be attributed to the effect of nanotube surface curvature on the overlap of the atomic *p*-orbitals. Nevertheless, such discrepancies did not significantly affect the reliability of our predictions for the electron transport properties of SWCNTs.

To quantify the deviations between the NTBM results presented in this section and their DFT counterparts, we employed the root mean square error (RMSE), calculated from the NTBM electron energies in the valence and conduction bands of the seven materials considered above relative to the corresponding DFT-calculated electronic states:

$$\mathrm{RMSE} = \sqrt{\frac{1}{N}\sum_{n,k}(U_{n,k}^{\mathrm{DFT}} - U_{n,k}^{\mathrm{NTBM}})^2}, \qquad (4)$$

where, for each system under study, the summation extends over all its $n = 2$ bands (valence and conduction bands) and over 121 k-points in the first Brillouin zone, with N denoting the total number of such points. The calculated RMSE values are summarized in Table 3. Equilibrium lattice constants a for nanotubes and hexagonal 2D structures are also presented in Table 3.

Table 3 reveals a considerable variation in RMSE values across different materials. The largest RMSE value (1.29 eV) was observed for graphene, which may be attributed to the specifics of NTBM parameterization for an ideal hexagonal carbon lattice. For graphane, the deviation of the NTBM-calculated EBS from the corresponding DFT data decreased (RMSE = 0.65 eV), yet remained relatively high, likely due to the presence of hydrogen bonds in this atomic structure, which are only weakly captured by the basic NTBM parameterization. The lowest RMSE value (0.11 eV) was obtained for γ1-graphyne-1, highlighting the good applicability of the NTBM approach discussed in this work for constructing EBSs of similar systems with pronounced sp^2 carbon hybridization. The two types of diamane (AA and AB) produced similar RMSE values (0.49 and 0.39 eV, respectively), demonstrating the robustness of this approach for exploring the EBSs of different carbon allotropic modifications. SWCNTs with different chirality yielded RMSE values in the range of 0.33 – 0.39 eV, further confirming the adequacy of NTBM modeling of the electronic properties of tubular carbon structures.

Thus, the NTBM described above demonstrates reasonably good accuracy (RMSE < 0.5 eV) in calculating the EBSs of carbon materials with moderate modifications of their crystal structures, such as graphyne, diamane, and nanotubes. Limited accuracy (RMSE > 0.5 eV) of this approach to quantum-mechanical modeling of electron transport properties appears to be characteristic of H–C systems subject to stronger external influences (e. g., adsorbed hydrogen atoms in graphane) or of idealized carbon structures such as graphene, where a more refined treatment of exchange interactions between atoms is likely required. Note that the NTBM parametrization presented here does not include non-electronic repulsion between ions and therefore cannot provide geometry of the considered systems. However, it is accurate enough to complement the classical MD studies of novel C and H–C nanoarchitectures [57, 58].

4. Conclusion

Over the past few decades, the methodologies and algorithms of computational materials science have undergone significant development. ML has addressed the challenge of interatomic potentials [59], while heuristic algorithms such as USPEX [60] have long been capable of successfully predicting the crystal structures of a wide range of systems. In this work, we have introduced a parameterized NTBM for predicting the electronic properties of various carbon and H–C atomic structures. This approach can support extensive searches for new materials of this type, as well as more

Table 3. RMSE values of the NTBM calculations of the EBSs of graphene, graphane, γ1-graphyne-1, (5,0) and (5,5) SWCNTs, and diamane with AA- and AB-type atomic stacking, relative to the corresponding DFT results. Equilibrium lattice constants a are also presented.

Material	Graphene	Graphane	γ1-graphyne-1	Diamane (AA)	Diamane (AB)	SWCNT (5,0)	SWCNT (5,0)
RMSE, eV	1.29	0.65	0.11	0.49	0.39	0.33	0.39
a, Å	2.47	2.54	6.89	2.52	2.53	4.26	2.47

efficient and accurate studies of the EBSs of their synthesized counterparts. The NTBM has demonstrated reasonably good predictive capability for the EBSs of materials with covalent bonding and localized electronic states, but it may require further parameterization for systems exhibiting pronounced electronic correlations. Ultimately, parameterization of the NTBM on the basis of DFT calculations overcomes the key limitation of the TB approach to quantum-mechanical modeling — its reliance on empirically fitted parameter values. This synthesis of methods allows the analytical advantages of TBM to be retained while complementing them with the accuracy of first-principles calculations.

***Conflicts of interest**: The authors declare no conflicts of interest.*

References

1. A. Demming, King of the elements? Nanotechnology. 21 (2010) 300201.
2. H.W. Kroto, J.R. Heath, S.C. O'Brien, R.F. Curl, R.E. Smalley, C_{60}: Buckminsterfullerene, Nature 318 (1985) 162–163.
3. X. Xu, R. Ray, Y. Gu, H.J. Ploehn, L. Gearheart, K. Raker, W.A. Scrivens, Electrophoretic Analysis and Purification of Fluorescent Single-Walled Carbon Nanotube Fragments, The Journal of the American Chemical Society 126 (2004) 12736–12737.
4. S. Iijima, Helical microtubules of graphitic carbon, Nature 354 (1991) 56–58.
5. A.M. Sladkov, Y.P. Kudryavtsev, Diamond, graphite, carbine — allotropic forms of carbon, Priroda 5 (1969) 37–44. (in Russian)
6. P.E. Eaton, T.W. Cole, Cubane, The Journal of the American Chemical Society. 86 (1964) 3157–3158.
7. K.S. Novoselov, A.K. Geim, S.V. Morozov, D.E. Jiang, Y. Zhang, S.V. Dubonos, I.V. Grigorieva, A.A. Firsov, Electric Field Effect in Atomically Thin Carbon Films, Science 306 (2004) 666–669.
8. S. Zhang, J. Zhou, Q. Wang, X. Chen, Y. Kawazoe, P. Jena, Penta-graphene: A new carbon allotrope, Proceedings of the National Academy of Sciences 112 (2015) 2372–2377.
9. S. Zhang, Q. Wang, X. Chen, P. Jena, Stable three-dimensional metallic carbon with interlocking hexagons, Proceedings of the National Academy of Sciences. 110 (2013) 18809–18813.
10. Q. Huang, D. Yu, B. Xu, W. Hu, Y. Ma, Y. Wang, Z. Zhao, B. Wen, J. He, Z. Liu, Y. Tian, Nanotwinned diamond with unprecedented hardness and stability, Nature 510 (2014) 250–253.
11. I.V. Krive, R.I. Shekhter, M. Jonson, Carbon "peapods" — a new tunable nanoscale graphitic structure, Low Temperature Physics 32 (2010) 887–905.
12. S. Piscanec, M. Lazzeri, J. Robertson, A.C. Ferrari, F. Mauri, Optical phonons in carbon nanotubes: Kohn anomalies, Peierls distortions, and dynamic effects, Physical Review B — Condensed Matter and Materials Physics 75 (2007) 035427.
13. Y. Ni, K.-L. Yao, H.-H. Fu, G.-Y. Gao, S.-C. Zhu, B. Luo, S.-L. Wang, R.-X. Li, The transport properties and new device design: the case of 6,6,12-graphyne nanoribbons, Nanoscale 5 (2013) 4468.
14. H. Terrones, M. Terrones, E. Hernandez, N. Grobert, J.-C. Charlier, P.M. Ajayan, New Metallic Allotropes of Planar and Tubular Carbon, Physical Review Letters 84 (2000) 1716.
15. M. Kociak, A.Y. Kasumov, S. Gueron, B. Reulet, I.I. Khodos, Y.B. Gorbatov, V.T. Volkov, L. Vaccarini, H. Bouchiat, Superconductivity in Ropes of Single-Walled Carbon Nanotubes, Physical Review Letters 86 (2001) 2416.
16. J. Liu, T. Zhao, S. Zhang, Q. Wang, A new metallic carbon allotrope with high stability and potential for lithium ion battery anode material, Nano Energy 38 (2017) 263–270.
17. H. Ohldag, T. Tyliszczak, R. Höhne, D. Spemann, P. Esquinazi, M. Ungureanu, T. Butz, π-Electron Ferromagnetism in Metal-Free Carbon Probed by Soft X-Ray Dichroism, Physical Review Letters 98 (2007) 187204.
18. C. Bergeret, J. Cousseau, V. Fernandez, J.-Y. Mevellec, S. Lefrant, Spectroscopic Evidence of Carbon Nanotubes' Metallic Character Loss Induced by Covalent Functionalization via Nitric Acid Purification, The Journal of Physical Chemistry C 112 (2008) 16411–16416.
19. L. Zhu, H. Hu, Q. Chen, S. Wang, J. Wang, F. Ding, Formation and electronic properties of hydrogenated few layer graphene, Nanotechnology 22 (2011) 185202.
20. D.C. Elias, R.R. Nair, T.M.G. Mohiuddin, S.V. Morozov, P. Blake, M.P. Halsall, A.C. Ferrari, D.W. Boukhvalov, M.I. Katsnelson, A.K. Geim, K.S. Novoselov, Control of Graphene's Properties by Reversible Hydrogenation: Evidence for Graphane, Science 323 (2009) 610–613.
21. H. Shi, L. Ding, D. Zhong, J. Han, L. Liu, L. Xu, P. Sun, H. Wang, J. Zhou, L. Fang, Z. Zhang, L.-M. Peng, Radiofrequency transistors based on aligned carbon nanotube arrays, Nature Electronics 4 (2021) 405.
22. Y. Lin, Y. Cao, S. Ding, P. Zhang, L. Xu, C. Liu, Q. Hu, C. Jin, L.-M. Peng, Z. Zhang, Scaling aligned carbon nanotube transistors to a sub-10 nm node, Nature Electronics 6 (2023) 506.
23. C. Xu, P. Ning, C. Luo, L. Cao, X. Deng, G. Zhou, Electronic properties and spintronic applications of r-N-graphyne nanoribbons, Physica E: Low-dimensional Systems and Nanostructures 136 (2022) 115003.
24. S. Pawar, H. Duadi, D. Fixler, Recent Advances in the Spintronic Application of Carbon-Based Nanomaterials, Nanomaterials 13 (2023) 598.
25. H. Wang, R. Zhou, D. Li, L. Zhang, G. Ren, L. Wang, J. Liu, D. Wang, Z. Tang, G. Lu, G. Sun, H.-D. Yu, W. Huang, High-Performance Foam-Shaped Strain Sensor Based on Carbon Nanotubes and $Ti_3C_2T_x$ MXene for the Monitoring of Human Activities, ACS Nano 15 (2021) 9690–9700.
26. H. Wang, Z. Zhao, P. Liu, X. Guo, Laser-Induced Graphene Based Flexible Electronic Devices, Biosensors 12 (2022) 55.
27. L.J. Sham, M. Schlüter, Density-Functional Theory of the Energy Gap, Physical Review Letters 51 (1983) 1888.
28. V.I. Anisimov, F. Aryasetiawan, A.I. Lichtenstein, First-principles calculations of the electronic structure and spectra of strongly correlated systems: the LDA+*U*

method, The Journal of Physics: Condensed Matter 9 (1997) 767.
29. J. Muscat, A. Wander, N. M. Harrison, On the prediction of band gaps from hybrid functional theory, Chemical Physics Letters. 342 (2001) 397 – 401.
30. J. Heyd, G. E. Scuseria, Efficient hybrid density functional calculations in solids: Assessment of the Heyd–Scuseria–Ernzerhof screened Coulomb hybrid functional, The Journal of Chemical Physics 121 (2004) 1187 – 1192.
31. R. Hoffmann, A. A. Kabanov, A. A. Golov, D. M. Proserpio, *Homo Citans* and Carbon Allotropes: For an Ethics of Citation, Angewandte Chemie International Edition 55 (2016) 10962 – 10976.
32. E. A. Belenkov, V. A. Greshnyakov, Classification schemes for carbon phases and nanostructures, New Carbon Materials 28 (2013) 273 – 282.
33. M. M. Maslov, K. P. Katin, High kinetic stability of hypercubane: Tight-binding molecular dynamics study, Chemical Physics Letters 644 (2016) 280 – 283.
34. A. Mostafaei, E. H. Semiromi, A tight-binding model for the electronic structure of MXene monolayers, Nanoscale 14 (2022) 11760 – 11769.
35. V. M. Pereira, A. H. Castro Neto, N. M. R. Peres, Tight-binding approach to uniaxial strain in graphene, Physical Review B — Condensed Matter and Materials Physics 80 (2009) 045401.
36. S. Banerjee, R. R. P. Singh, V. Pardo, W. E. Pickett, Tight-Binding Modeling and Low-Energy Behavior of the Semi-Dirac Point, Physical Review Letters 103 (2009) 016402.
37. J. C. Slater, G. F. Koster, Simplified LCAO Method for the Periodic Potential Problem, Physical Review 94 (1954) 1498.
38. M. S. Tang, C. Z. Wang, C. T. Chan, K. M. Ho, Environment-dependent tight-binding potential model, Physical Review B 53 (1996) 979.
39. T. Yamashita, N. Sato, H. Kino, T. Miyake, K. Tsuda, T. Oguchi, Crystal structure prediction accelerated by Bayesian optimization, Physical Review Materials 2 (2018) 013803.
40. Y. Zhuo, A. Mansouri Tehrani, J. Brgoch, Predicting the Band Gaps of Inorganic Solids by Machine Learning, The Journal of Physical Chemistry Letters 9 (2018) 1668 – 1673.
41. A. C. Rajan, A. Mishra, S. Satsangi, R. Vaish, H. Mizuseki, K.-R. Lee, A. K. Singh, Machine-Learning-Assisted Accurate Band Gap Predictions of Functionalized MXene, Chemistry of Materials 30 (2018) 4031 – 4038.
42. K. T. Schütt, M. Gastegger, A. Tkatchenko, K.-R. Müller, R. J. Maurer, Unifying machine learning and quantum chemistry with a deep neural network for molecular wavefunctions, Nature Communications 10 (2019) 5024.
43. G. Fan, A. McSloy, B. Aradi, C.-Y. Yam, T. Frauenheim, Obtaining Electronic Properties of Molecules through Combining Density Functional Tight Binding with Machine Learning, The Journal of Physical Chemistry Letters 13 (2022) 10132 – 10139.
44. H. Li, Z. Wang, N. Zou, M. Ye, R. Xu, X. Gong, W. Duan, Y. Xu, Deep-learning density functional theory Hamiltonian for efficient ab initio electronic-structure calculation, Nature Computational Science 2 (2022) 367 – 377.
45. Q. Gu, Z. Zhouyin, S. K. Pandey, P. Zhang, L. Zhang, W. E, Deep learning tight-binding approach for large-scale electronic simulations at finite temperatures with ab initio accuracy, Nature Communications. 15 (2024) 6772.
46. A. S. Rosen, S. M. Iyer, D. Ray, Z. Yao, A. Aspuru-Guzik, L. Gagliardi, J. M. Notestein, R. Q. Snurr, Machine learning the quantum-chemical properties of metal–organic frameworks for accelerated materials discovery, Matter 4 (2021) 1578 – 1597.
47. L. A. Openov, A. I. Podlivaev, Insulator band gap in graphane nanoribbons, Semiconductors 45 (2011) 633 – 635.
48. V. Prudkovskiy, M. Berd, E. Pavlenko, K. Katin, M. Maslov, P. Puech, M. Monthioux, W. Escoffier, M. Goiran, B. Raquet, Electronic coupling in fullerene-doped semiconducting carbon nanotubes probed by Raman spectroscopy and electronic transport, Carbon 57 (2013) 498 – 506.
49. V. B. Merinov, V. A. Domnin, Effect of Structural Defects and Adsorbates on the Ballistic Conductivity of Carbon Nanotubes, Russian Journal of Physical Chemistry B 17 (2023) 215 – 221.
50. K. P. Katin, M. M. Maslov, Thermal stability of nitro derivatives of hydrocarbon cubane, Russian Journal of Physical Chemistry B 5 (2011) 770 – 779.
51. M. M. Maslov, A. I. Podlivaev, K. P. Katin, Nonorthogonal tight-binding model with H–C–N–O parameterization, Molecular Simulation 42 (2016) 305 – 311.
52. D. Vanderbilt, Soft self-consistent pseudopotentials in a generalized eigenvalue formalism, Physical Review B 41 (1990) 7892.
53. P. Hohenberg, W. Kohn, Inhomogeneous Electron Gas, Physical Review 136 (1964) B864.
54. W. Kohn, L. J. Sham, Self-Consistent Equations Including Exchange and Correlation Effects, Physical Review 140 (1965) A1133.
55. J. M. Renders, S. P. Flasse, Hybrid methods using genetic algorithms for global optimization, IEEE Transactions on Systems, Man, and Cybernetics, Part B (Cybernetics) 26 (1996) 243 – 258.
56. V. A. Kulbachinsky, Physics of Nanosystems, Physmathlit, Moscow, 2023, 513 – 515 pp. (in Russian)
57. P. V. Polyakova, L. K. Galiakhmetova, R. T. Murzaev, D. S. Lisovenko, J. A. Baimova, Elastic properties of diamane, Letters on Materials 13 (2023) 171–176.
58. N. G. Apkadirova, K. A. Krylova, J. A. Baimova, Effect of external pressure on the hydrogen storage capacity of a graphene flake: molecular dynamics, Letters on Materials 12 (2022) 445 – 450.
59. H. Gokcan, O. Isayev, Learning molecular potentials with neural networks, Wiley Interdisciplinary Reviews: Computational Molecular Science 12 (2022) e1564.
60. A. O. Lyakhov, A. R. Oganov, H. T. Stokes, Q. Zhu, New developments in evolutionary structure prediction algorithm USPEX, Computer Physics Communications 184 (2013) 1172 – 1182.